

This article appeared in a journal published by Elsevier. The attached copy is furnished to the author for internal non-commercial research and education use, including for instruction at the authors institution and sharing with colleagues.

Other uses, including reproduction and distribution, or selling or licensing copies, or posting to personal, institutional or third party websites are prohibited.

In most cases authors are permitted to post their version of the article (e.g. in Word or Tex form) to their personal website or institutional repository. Authors requiring further information regarding Elsevier's archiving and manuscript policies are encouraged to visit:

<http://www.elsevier.com/copyright>



Potential of mean force for human lysozyme–camelid vhh hl6 antibody interaction studies

Yeng-Tseng Wang^{a,b,*}, Jun-Min Liao^b, Cheng-Lung Chen^b, Zhi-Yuan Su^c,
Chang-Hung Chen^a, Jeu-Jiun Hu^d

^a National Center for High-performance Computing, Hsin-Shi, Tainan County, Taiwan

^b The Department of Chemistry, National Sun Yat-Sen University, Kaohsiung 804, Taiwan

^c The Department of Information Management, Chia Nan University of Pharmacy and Science, Tainan 717, Taiwan

^d The Department of Information Management, SHU-TE University, Kaohsiung 804, Taiwan

Received 8 August 2007; in final form 1 February 2008

Available online 7 February 2008

Abstract

Calculating antigen–antibody interaction energies is crucial for understanding antigen–antibody associations in immunology. To shed further light into this equation, we study a separation of human lysozyme–camelid vhh hl6 antibody (cAb-HuL6) complex. The c-terminal end-to-end stretching of the lysozyme–antibody complex structures have been studied using potential of mean force (PMF) calculations based on molecular dynamics (MD) and explicit water model. For the lysozyme–antibody complex, there are six important intermediates in the c-terminal extensions process. Inclusion of our simulations may help to understand the binding mechanics of lysozyme–cAb-HuL6 antibody complex.

© 2008 Elsevier B.V. All rights reserved.

1. Introduction

Stretching mechanics is an important factor for understanding antigen–antibody associations and improving the binding efficiency of antigen–antibody in immunology. Amyloids are insoluble fibrous protein aggregations sharing specific structural features. Amyloid diseases, such as Alzheimer's disease (AD) and Parkinson's disease [1], are characterized by an aberrant assembly of specific proteins or protein fragments into fibrils and plaques that are deposited in various tissues and organs. From *in vitro* experiments, Dumoulin et al. [2] shows that the cAb-HuL6 antibody fragments [3] are able to inhibit the aggregations of human lysozyme proteins. The cAb-HuL6 anti-

body is a fragment of heavy-chain camel antibody with high specificity for human lysozyme. The three dimensional structure of lysozyme–cAb-HuL6 antibody complex structure is available from Dumoulin et al. [2]

The PMF calculations of stretching lysozyme–antibody complex from equilibrium MD simulations have been performed with umbrella sampling techniques and the weighted histogram analysis method (WHAM). Computations on the c-terminal end-to-end extensions of lysozyme–antibody complex have been performed in explicit TIP3P [4] water model with particle mesh Ewald (PME) [5] and shifted electrostatic functions (non-PME). The distance of the extension is from 6.3 nm to 16.8 nm.

The present study performs MD simulations on model systems of lysozyme–antibody complex structures on c-terminal end-to-end extensions. Detailed analysis of the MD simulations reveals the PMF, the profile of cumulative changes in dihedral angles (CCDAs), and inter-protein molecular hydrogen bonds (IPMHBS) in the c-terminal extensions process.

* Corresponding author. Address: National Center for High-performance Computing, Hsin-Shi, Tainan County, Taiwan. Fax: +886 5050945.

E-mail address: cs00jsw00@nchc.org.tw (Y.-T. Wang).

2. Methods

Many lysozyme–antibody complex structures have been solved and deposited in protein data banks. We used the X-ray structure of human lysozyme–cAb-HuL6 antibody complex (PDB ID: 1OP9) as the lysozyme–antibody model in our simulations because the interactions of the complex structures have been well studied by Dumoulin [1]. This model is shown in Fig. 1.

Calculations were performed with the performed with the program Amber [6] and NAMD [7] using the amber ff99 all-hydrogen amino acid parameters and explicit TIP3P water model. The initial structure of lysozyme–antibody was overlaid with a pre-equilibrated solvent box of the TIP3P water model (the solvent box size is $15.4 \times 13.5 \times 7.5 \text{ nm}^3$) and chloride ions. All water molecules within 0.19 nm of lysozyme–antibody atoms were deleted and chorine ions added at random positions in the box as needed to render the system electrostatically neutral. The simulation system size is $15.4 \times 13.5 \times 7.5 \text{ nm}^3$ and includes 48183 TIP3P water molecules. All MD simulations were performed in the isobaric, isothermal ensemble [8] (the simulation temperature is equal to 310 K), unless noted, using the verlet integrator, an integration time step of 0.002 ps and SHAKE [9] of all covalent bonds involving hydrogen atoms. In electrostatic interactions, atoms based truncation individually using PME method and non-PME method. And the switch van der

Waals functions was also used with a 1.8 nm cutoff for atom-pair lists. The complex structures were minimized for 10000 conjugate gradient steps. The minimized complex structures were then subjected to a 1 ns isothermal, constant volume MD simulation. The final structures from these simulations were used to initiate the PMF calculations.

PMF calculations of studying the c-terminal end-to-end extensions of the complex structures used a reaction coordinate defined as the c-terminal CA atom of the lysozyme to the c-terminal CA atom of the antibody distance (r). The r value for the lysozyme–antibody complex was varied from 6.3 nm to 16.8 nm in 0.5 nm increments. MD simulations for PMF determination were performed with an initial 0.4 ns equilibration followed by 0.8 ns of sampling at a given distance (r). The harmonic distance constraint was then increased by 0.5 nm for the next 0.4 ns of equilibrium and 0.8 ns of sampling performed. Calculations of the PMF were performed using the WHAM method [10] and WHAM was explained in Allen et al. [11].

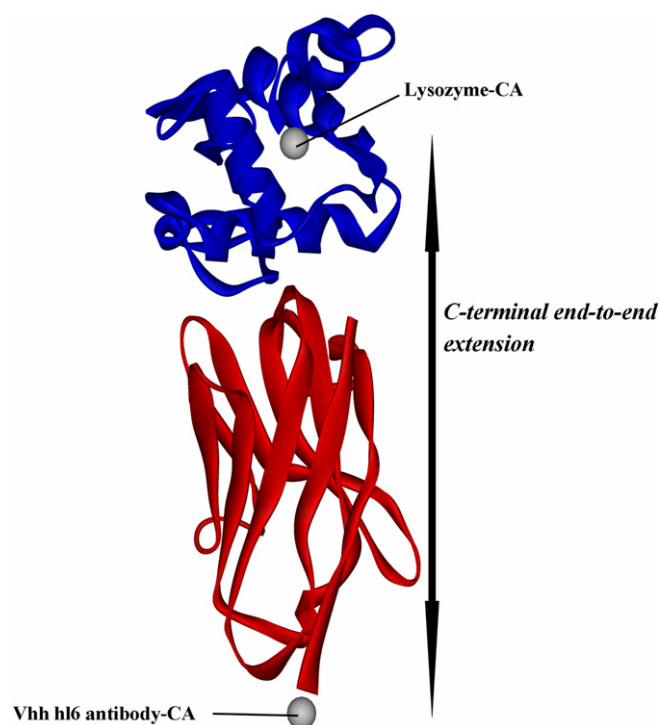


Fig. 1. Model for the simulation of c-terminal end-to-end extension on human lysozyme–camelid vhh hl6 antibody complex. c-Terminal end-to-end: distance between the CA atom (Lysozyme: 130th valine residue) and the CA atom (Vhh hl6 antibody: 251th serine residue).

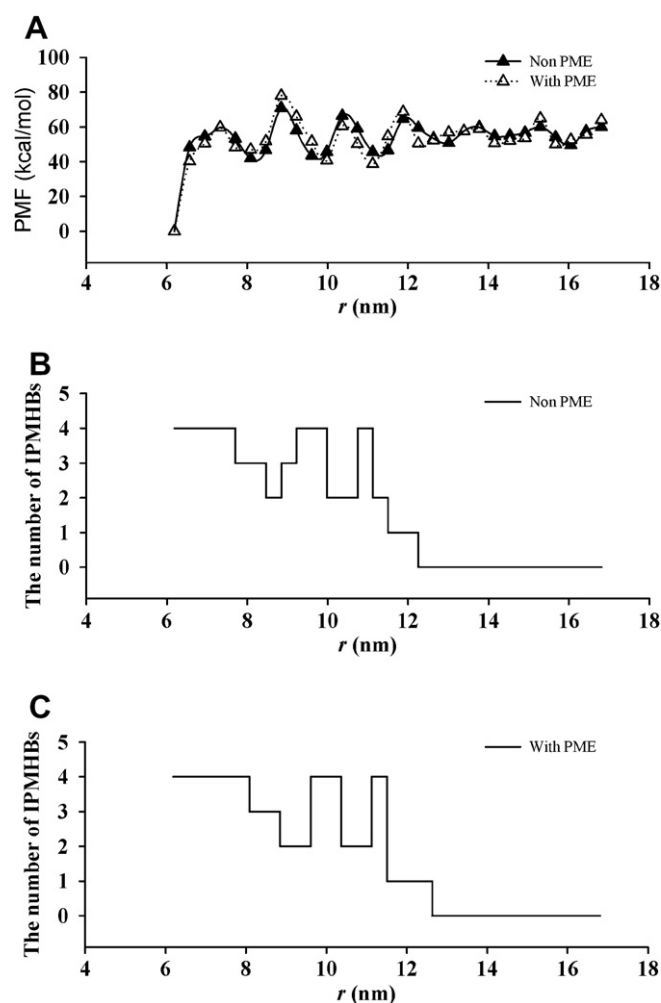


Fig. 2. (A) Calculated PMF with non-PME and PME methods. (B) and (C) the number of inter-protein molecular hydrogen bonds for the extension for the value of r from 6.3 nm through 16.8 nm. Here r refers to the distance of the c-terminal end-to-end extensions.

3. Results and discussion

Fig. 2A shows the free energy profiles with PME and non-PME treatments for r of the lysozyme–antibody complex structure from 6.3 nm to 16.8 nm. The complex structures were extended from 6.3 nm to 16.8 nm and out to produce four large energy barriers at r of 7.32, 9.22, 10.36, and 11.87 nm. Two numbers of lower energy barriers (less than 10 kcal/mol) were presented in the free energy profile with r of 13.77 and 15.29 nm. Fig. 2B and C shows the profiles of IPMHBs from tracing r of 6.3–16.8 nm for the electrostatic interactions with PME and non-PME treatments. The complex structures were extended from 6.3 nm to 16.8 nm and out to produce two sag at r of

8.3–9.8 and 9.8–11.8 nm. During the c-terminal extensions process at r of 12.8–16.8 nm, the number of IPMHBs was decreased to zero. Figs. 3 and 4 show the profiles of CCDAs from tracing r of 6.3–16.8 nm. In Figs. 3 and 4, the CCDAs of amino residues (15th Glycine, 39th Glycine, 169th Glycine and 249th Cystein) were obvious in phi angle. And the CCDAs of 62th–73th, 110th–120th, and 247th–250th amino residues were obvious in psi angles.

Then the CCDAs and IPMHBs with PME and non-PME treatments were individually traced in r of 6.3–8.0, 8.0–9.9, 9.9–11.5, 11.5–13.0, 13.0–14.1, and 14.1–16.0 nm (the range of energy barriers). The amino residues which CCDAs were more than 300 degree (in phi or psi angles) were shown in Table 1. When the lysozyme–antibody c-ter-

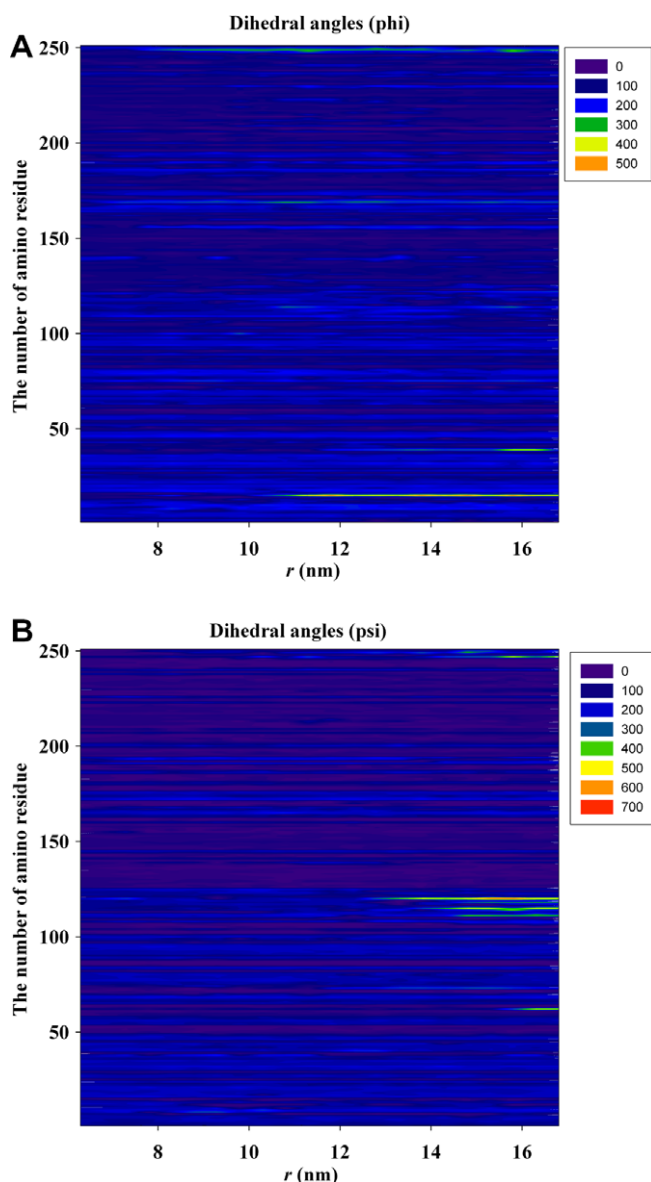


Fig. 3. A profile of cumulative changes in dihedral angles (phi and psi) with non-PME method for the value of r from 6.3 nm through 16.8 nm. Here no. of amino residues: 1–121 (lysozyme) and 121–251 (camelid vhh hl6 antibody).

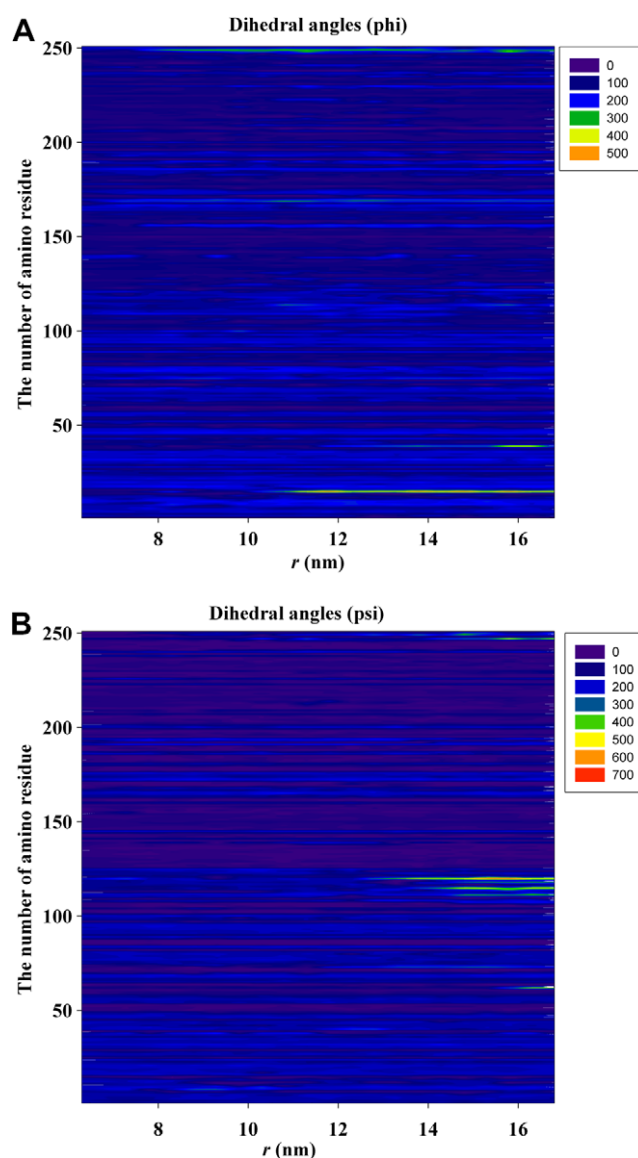


Fig. 4. A profile of cumulative changes in dihedral angles (phi and psi) with PME method for the value of r from 6.3 nm through 16.8 nm. Here no. of amino residues: 1–121 (lysozyme) and 121–251 (camelid vhh hl6 antibody).

minimal extensions system strode across the first energy barrier (r of 6.3–8.0 nm), the 120th serine was rotated more than 300 degree in psi angle and the complex structures maintained four IPMHBs. As the complex structures strode across the second energy barrier (r of 8.0–9.9 nm), there were obvious variation in dihedral angles of 8th Glycine and 249th Cysteine. In the PMF profiles, the value (equal to 78.05 kcal/mol) of the second barrier height with PME treatments was greater than the one (equal to 71.05 kcal/mol) with non-PME treatments. In the PME and non-PME treatments barrier height, there were individually two and three IPMHBs. In the third energy barrier (r of 9.9–11.5 nm), the three amino residues (15th Glycine, 169th Glycine, and 249th Cysteine) were rotated more than 300 degree in dihedral angles and there were still two IPMHBs in the barrier height. In r of 11.1 nm, the PMF (equal to 38.74 kcal/mol) with PME treatments was lower than the one (equal to 45.74 kcal/mol) with non-PME treatments and the IPMHBs (four IPMHBs) with PME treatments were greater than the one (two IPMHBs) with non-PME treatments. In the fourth energy barrier (r of 11.5–13.0 nm), the dihedral angles of the amino residues

(15th Glycine, 120th Serine, and 249th Cysteine) were rotated more than 300 degree, especially the 15th Glycine which the psi angle was rotate 577 degree in non-PME treatments and 537 degree in PME treatments. And there were two IPMHBs in the fourth barrier height. In the last two lower energy barriers, there were four amino residues (15th Glycine, 120th Serine, 115th Threonine, and 247th Glutamine) with large variation (rotated more than 400 degree) in psi or phi angles, especially the 120th Serine which the psi angle was individually rotated more than 500° in PME and non-PME treatments. And there was no IPMHBs in the last two barriers.

Our simulation results suggested that when the cAb-HuL6 antibody was close to the lysozyme protein, the four amino residues (15th Glycine, 120th Serine, 115th Threonine, and 247th Glutamine) play important roles in relaxing the lysozyme and antibody structures and maked the antibody–lysozyme easy to bind together. After the binding of the antibody–lysozyme, the 15th Glycine was still a key point which relaxed the protein structures and more inter-protein molecular hydrogen bonds might help the complex structures stride across energy barriers more easily.

4. Conclusion

In this Letter, we propose that using the c-terminal end-to-end extensions of the cAb-HuL6 antibody–lysozyme complex structures (r) with PME and non-PME treatments to predict the binding mechanics and the free energy profile. We carried out c-terminal extensions MD simulations of the antibody–lysozyme structures. We used WHAM method to extract the free energy profile from the MD simulations and found six important energy barriers in the c-terminal extensions process. In this work we used cumulative changes in dihedral angles and inter-protein molecular hydrogen bonds to analysis the energy barriers and found that the four amino residues (15th Glycine, 120th Serine, 115th Threonine, and 247th Glutamine) and the number of inter-protein molecular hydrogen bonds might be important in the development of bioactive antibody analogues.

Acknowledgments

This work was supported by the National Center for High-performance Computing and the National Sun Yat-Sen university, Taiwan.

References

- [1] E.H. Koo, P.T. Lansbury, J.W. Kelly, Proc. Natl. Acad. Sci. 96 (1999) 9989.
- [2] M. Dumoulin et al., Nature 424 (2003) 783.
- [3] M. Dumoulin et al., Protein Sci. 11 (2002) 500.
- [4] W.L. Jorgensen, J. Chandrasekhar, J.D. Madura, R.W. Impey, M.L. Klein, J. Chem. Phys. 79 (1983) 926.
- [5] T. Darden, D. York, L. Pederson, J. Chem. Phys. 98 (1993) 10089.

Table 1

The amino residues which CCDAs are more than 300° in the range of 12.3–16.8, 9.6–12.3, and 6.8–9.8 nm (r) with PME and non-PME treatments

r (nm)	No. of amino residue	Cumulative changes in dihedral angles/degree			
		Non-PME		PME	
		Phi (Φ)	Psi (Ψ)	Phi (Φ)	Psi (Ψ)
6.3–8.0	120th Serine	58.00	301.00	48.00	316.00
	8th Glycine	95.00	324.00	92.00	329.00
	249th Cysteine	310.00	166.00	314.00	161.00
9.9–11.5	15th Glycine	464.00	26.00	468.00	20.00
	169th Glycine	316.00	49.00	324.00	32.00
	249th Cysteine	308.00	204.00	325.00	229.00
11.5–13.0	15th Glycine	577.00	70.00	537.00	85.00
	120th Serine	124.00	325.00	128.00	342.00
	249th Cysteine	307.00	204.00	321.00	216.00
13.0–14.1	15th Glycine	568.00	51.00	582.00	65.00
	73th Lysine	137.00	314.00	129.00	331.00
	115th Threonine	47.00	313.00	57.00	325.00
	120th Serine	155.00	515.00	147.00	532.00
	249th Cysteine	278.00	325.00	264.00	304.00
14.1–16.0	15th Glycine	573.00	62.00	541.00	74.00
	39th Glycine	391.00	42.00	374.00	51.00
	62th Lysine	42.00	312.00	31.00	334.00
	73th Lysine	137.00	339.00	147.00	342.00
	111th Tryptophan	118.00	387.00	114.00	371.00
	115th Threonine	108.00	498.00	124.00	491.00
	118th Threonine	148.00	332.00	142.00	347.00
	120th Serine	135.00	703.00	145.00	716.00
	247th Glutamine	61.00	484.00	57.00	479.00
	248th Glycine	318.00	17.00	342.00	25.00
	249th Cysteine	308.00	195.00	324.00	187.00

The number of residue: 1–121 (lysozyme), 121–251 (camelid vhh hl6 antibody).

- [6] D.A. Case et al., *J. Comput. Chem.* 26 (2005) 1668.
- [7] M. Nelson, W. Humphrey, A. Gursoy, A. Dalke, L. Kale, R.D. Skeel, K. Schulten, *J. Supercomput. Appl.* 10 (1996).
- [8] S.E. Feller, Y. Zhang, R.W. Pastor, *J. Chem. Phys.* 103 (1995) 4613.
- [9] J.P. Ryckaert, G. Ciccotti, H.J.C. Berendsen, *J. Comput. Phys.* 23 (1977) 327.
- [10] M. Souaille, B. Roux, *Comput. Phys. Commun.* 135 (2001) 40.
- [11] T.W. Allen, T. Bastung, S. Kuyucak, S.H. Chung, *Biophys. J.* 84 (2003) 2159.